The relation between the melt topology and glass-forming ability for liquid Ge-Se alloys

The relation between the melt topology and glass-forming ability for liquid Ge–Se alloys

Philip S Salmon and Jian Liu

School of Physics, University of East Anglia, Norwich NR4 7TJ, UK

Abstract. The topology of liquid Ge_ySe_{1-y} ($0 \leqslant y \leqslant 1$) alloys, at the compositions $y = 0.33$, 0.4, 0.5 and 1, is studied using neutron diffraction to measure the Bhatia–Thornton number–number partial structure factor $S_{NN}(kr_1)$, where k and r_1 are, respectively, the scattering vector and nearest-neighbour distance in real space. $S_{NN}(kr_1)$ has, for the range $0 \leqslant kr_1 \leqslant 10$, a prominent three-peak character in the case of the glass-forming melt $GeSe_2$ ($y = 0.33$). This character changes significantly with increasing y: the so-called first sharp diffraction peak (FSDP) is virtually eliminated at $y = 0.5$, a composition for which the amorphous state is not formed by usual bulk-quenching methods, and the third peak becomes a shoulder to the second at $y = 1$. The concomitant changes on both the short and intermediate real-space length scales are discussed in terms of a break-up of the $GeSe_2$ network structure. It is found that liquid GeSe is not characterized by a regular octahedral coordination environment but that it is topologically similar to liquid As.

1. Introduction

The object of this paper is to investigate the relation between the *melt* topology and glass forming ability of three alloys in the Ge–Se system, namely GeSe, $GeSe_{1.5}$ and $GeSe_2$, by using neutron diffraction to measure the Bhatia–Thornton (BT) (1970) number–number partial structure factor, $S_{NN}(k)$, where k is the scattering vector. The Ge_ySe_{1-y} ($0 \leqslant y \leqslant 1$) system was chosen for investigation since it is a much studied proto-typical glass former. The composition range for which bulk quenched glasses can be made is large, covering $0 \leqslant y \leqslant 0.42$ (Tronc *et al* 1973, Azoulay *et al* 1975). Hence, as Ge is added to $GeSe_2$ to give $GeSe_{1.5}$ ($y = 0.4$) and GeSe ($y = 0.5$), the ability of the system to form glasses diminishes and it is of interest to find the accompanying change in the structure of the melt, especially since a wide range of experiments show that there is a significant change in the nature of the bonding. For example, as the Ge composition is increased from $y = 0.33$ to $y = 0.5$ at 750 °C the electrical resistivity decreases by approximately four orders of magnitude (Haisty and Krebs 1969, Ruska and Thurn 1976), the molar volume decreases by a factor of 1.24 (Ruska and Thurn 1976) and the adiabatic compressibility decreases by a factor of 2.9 (Tsuchiya 1990). For the same change of composition at 900 °C, the kinematic viscosity decreases by a factor of approximately two (Glazov and Situlina 1969, Ruska and Thurn 1976). As y is increased further to $y = 1$ the alloys become metallic (see e.g. Uemura *et al* 1976).

In a neutron diffraction experiment on Ge–Se alloys the complexity of correlations associated with the measured total structure factor, $F(k)$, is reduced to the single partial structure factor $S_{NN}(k)$ since the coherent neutron scattering lengths of naturally occurring Ge and Se are comparable. This is of particular interest because $F(k)$ for many binary

glasses of the type M_yX_{1-y} displays a characteristic three-peak structure (Wright *et al* 1985) for $0 \leqslant kr_1 \leqslant 10$, where r_1 is the nearest-neighbour distance, whose origin can be traced to $S_{NN}(k)$ (Salmon 1992). Since the Fourier transform of this function, the partial pair distribution function $g_{NN}(r)$, describes the average sites of the scattering species but is not concerned with the nature of the chemical species that decorate those sites, it gives information on the topology of the system. The first of the three peaks in $F(k)$, which is often referred to as the 'first sharp diffraction peak' (FSDP), occurs at low kr_1 values of between $\simeq 2.1$ and $\simeq 3.1$ for a wide variety of oxide, halide and chalcogenide disordered systems (Price *et al* 1988) and is a prominent feature for both the liquid (Uemura *et al* 1978, Susman *et al* 1990, Penfold and Salmon 1990, 1991) and glassy (Uemura *et al* 1975, Wright *et al* 1985, Feltz *et al* 1985, Fuoss and Fischer-Colbrie 1988, Susman *et al* 1990, Fischer-Colbrie and Fuoss 1990) phases of GeSe$_2$. The FSDP pertains to the intermediate-range order (IRO) in the system and is usually taken to be a signature that the bonding takes a significant directional character. The present experiments on Ge–Se alloys will therefore yield information on the topology at *both* short and intermediate length scales.

2. Theory

In a neutron diffraction experiment on Ge$_y$Se$_{1-y}$ the total structure factor $F(k)$ derived from the coherent scattering can be expressed as

$$F(k) = \langle b \rangle^2 [S_{NN}(k) - 1] + y(1-y)(b_{Ge} - b_{Se})^2 [\{S_{CC}(k)/y(1-y)\} - 1]$$
$$+ 2\langle b \rangle (b_{Ge} - b_{Se}) S_{NC}(k) \tag{1}$$

where

$$\langle b \rangle = y b_{Ge} + (1-y) b_{Se} \tag{2}$$

and b_α is the coherent scattering length of chemical species α. $S_{NN}(k)$, $S_{CC}(k)$ and $S_{NC}(k)$ are, respectively, the BT number–number, concentration–concentration and number–concentration partial structure factors (Bhatia and Thornton 1970).

The real-space interpretation of $F(k)$ is obtained by Fourier transformation:

$$G(r) = \frac{1}{2\pi^2 n_o r} \int_0^\infty F(k) k \sin(kr) \, dk = \langle b \rangle^2 [g_{NN}(r) - 1] + y(1-y)(b_{Ge} - b_{Se})^2 g_{CC}(r)$$
$$+ 2y(1-y)\langle b \rangle (b_{Ge} - b_{Se}) g_{NC}(r) \tag{3}$$

where n_0 is the total number density of particles in the system and the $g_{\alpha\beta}(r)$ are the BT partial pair distribution functions. In the case when $b_{Ge} = b_{Se}$, equation (1) can be rewritten as

$$S_{NN}(k) - 1 = F(k)\langle b \rangle^{-2} \tag{4}$$

which is also valid for pure Ge ($y = 1$) or Se ($y = 0$).

In terms of the Faber–Ziman partial structure factors, $A_{\alpha\beta}(k)$, equation (4) becomes

$$S_{NN}(k) - 1 = y^2 A_{GeGe}(k) + (1-y)^2 A_{SeSe}(k) + 2y(1-y) A_{GeSe}(k) \tag{5}$$

where the corresponding partial pair distribution functions $g'_{\alpha\beta}(r)$ are given by

$$g'_{\alpha\beta}(r) = 1 + \frac{1}{2\pi^2 n_0 r} \int_0^\infty [A_{\alpha\beta}(k) - 1] k \sin(kr) \, dk. \tag{6}$$

The mean number of particles of type β contained in a volume defined by two concentric spheres of radii r_1 and r_2, centred on a particle of type α, is given by

$$\bar{n}_\alpha^\beta = 4\pi n_o c_\beta \int_{r_1}^{r_2} r^2 g_{\alpha\beta}'(r)\, \mathrm{d}r \tag{7}$$

where c_β is the atomic fraction of species β ($c_{Ge} = y$, $c_{Se} = (1 - y)$). Hence the average coordination number, *irrespective* of the species type, is given by

$$\bar{n} = 4\pi n_0 \int_{r_1}^{r_2} r^2 g_{NN}(r)\, \mathrm{d}r = c_{Ge}\left(\bar{n}_{Ge}^{Ge} + \bar{n}_{Ge}^{Se}\right) + c_{Se}\left(\bar{n}_{Se}^{Se} + \bar{n}_{Se}^{Ge}\right). \tag{8}$$

3. Experiment

The experiment on liquid $GeSe_2$ at 784(3) °C was performed using the D4B diffractometer at the Institut Laue–Langevin, Grenoble, and is described elsewhere (Penfold and Salmon 1990, 1991). The $GeSe_{1.5}$ and GeSe samples were made by mixing elemental Ge lumps (99.9999%, Aldrich) and Se pellets (99.999+%, Aldrich) in silica ampoules that had been cleaned using chromic acid prior to etching with a 40% solution of hydrofluoric acid (for further details see Penfold and Salmon 1989). The sample-filled ampoules were evacuated to a pressure of $\sim 10^{-5}$ Torr for appproximately 24 h, purged with helium gas and sealed under vacuum prior to being slowly heated in a rocking furnace to a temperature of 800 °C where they were held for approximately 30 h. The samples were then cooled slowly to room temperature and transferred to matched cylindrical silica tubes of internal radius 3.52(1) mm and wall thickness 1.07(1) mm ready for the neutron diffraction experiments. The latter were made using the LAD instrument at the ISIS pulsed neutron source, Rutherford Appleton Laboratory.

The complete LAD diffraction experiment comprised the measurement of an empty cylindrical vanadium heater, the samples contained in silica cells in the heater at 728(3) °C, an empty silica cell in the heater at 693(3) °C, a vanadium rod of radius 4.154(8) mm for normalization purposes and nothing placed at the sample position in order to estimate the background scattering. The data analysis was performed using the ATLAS suite of programs (Soper *et al* 1989). Measured values were used for the wavelength-dependent total cross-sections of silica and vanadium. The sample total cross-sections were calculated using the values of Sears (1992). The liquidus occurs at 742(2) °C for $y = 0.33$ and 668(2) °C for $y = 0.4$. Its value for $y = 0.5$ is more difficult to determine (Ipser *et al* 1982) but lies between the incongruent melting point of 675 °C and the temperature of the present experiment, i.e. 728(3) °C.

LAD comprises 14 groups of detectors at scattering angles of $\pm 5°$, $\pm 10°$, $\pm 20°$, $\pm 35°$, $\pm 60°$, $\pm 90°$ and $\pm 150°$ corresponding to instrumental resolution functions ($\Delta k/k$) of 11, 6, 2.8, 1.7, 1.2, 0.8 and 0.5% respectively. The final $F(k)$ functions were constructed by merging all those diffraction patterns from the different groups that showed good agreement. In the region of the FSDP (~ 1 Å^{-1}) the $F(k)$ were dominated by the $\pm 20°$ and $\pm 35°$ detector banks. Hence the resolution broadening of $F(k)$ in this region of k space is comparable to that for the $F(k)$ of liquid $GeSe_2$ (for D4B $\Delta k/k \simeq 2\%$, Blank and Maier 1988). It was checked (Salmon and Benmore 1992) that the final $F(k)$ functions tend to the correct high-k limit, obey the usual sum rule relation and that there is good overall agreement between $F(k)$ and the back-Fourier transform of $G(r)$ after the unphysical low-r oscillations are set to their calculated limiting value of $G(0) = -\langle b \rangle^2$. For the GeSe and $GeSe_{1.5}$ samples these

criteria were met by using, in the data analysis, effective number densities which were, respectively, 15 and 7% lower than those given in the literature (Ruska and Thurn 1976). The reason for this discrepancy, which is a typical problem associated with high-temperature experiments (see, e.g., Salmon 1988, Jal *et al* 1990), could not be unequivocally traced but may result from small bubbles in the viscous liquid samples. The number densities used for Fourier transforming and calculating the coordination numbers were taken from the data of Ruska and Thurn (1976) and are given in table 1.

Table 1. Weighting factors for the Bhatia–Thornton partial structure factors (equation (1)) and some other experimental parameters.

Melt	y	$\langle b \rangle^2$ (barn^2)	$y(1-y)(b_{Ge}-b_{Se})^2$ (barn^2)	$2\langle b \rangle(b_{Ge}-b_{Se})$ (barn^2)	T (°C)	n_0 (Å^{-3})
GeSe$_2$	0.33	0.6467	0.0001	0.0346	784(3)	0.0311(2)
GeSe$_{1.5}$	0.40	0.6490	0.0001	0.0346	728(3)	0.0336(2)
GeSe	0.50	0.6525	0.0001	0.0347	728(3)	0.0387(2)
Ge	1.00	0.6699	0	0	1000(3)	0.0456(3)

4. Results

The measured $F(k)$ are dominated by $S_{NN}(k)$ as shown by the weighting factors of the $S_{\alpha\beta}(k)$ (see table 1), which were calculated using $b_{Ge} = 8.185(20)$ fm and $b_{Se} = 7.970(9)$ fm (Sears 1992). The number–number partial structure factors were therefore obtained using equation (4) and are plotted in figure 1 as a function of kr_1, where r_1 is the position of the first peak in $g_{NN}(r)$ (see table 2). The data satisfy the required inequality relation $S_{NN}(k) > 0$ (see, e.g., Parrinello and Tosi 1979) and the good agreement between $S_{NN}(k)$ and the Fourier back-transform of the corresponding $g_{NN}(r)$, after the unphysical low-r oscillations have been set equal to their limiting value ($g_{NN}(0) = 0$), attests to the absence of substantial systematic errors. For example, no peak is observed in $g_{NN}(r)$ at the Si–O bond distance of 1.61 Å (Grimley *et al* 1990), which confirms that the silica container correction has been properly made. The thermodynamic limit $S_{NN}(0)$ (Bhatia and Thornton 1970) could not be calculated for comparison with the neutron data because insufficient information is available in the literature.

The real-space functions are given in figure 2 in terms of the variable r/r_1. They were obtained both by direct Fourier transformation of $S_{NN}(k)$ and by the minimum information method (MIM) of Soper (1990). The data for liquid Ge at 1000 °C (Salmon 1988) are also presented in figures 1 and 2 to provide a comparison with the Ge-Se alloy results. The melting point of Ge is 937 °C (Ipser *et al* 1982).

5. Discussion

5.1. The number–number partial structure factor $S_{NN}(k)$

It is clear from figure 1 that there is a substantial change in the topology of the melt as the Ge content is increased from $y = 0.33$ to $y = 1$. For example, the second peak in $S_{NN}(k)$ at k_2 becomes the highest entity (table 2); the FSDP located at k_1 is eliminated; the second and third peaks shift towards each other with the latter becoming a shoulder at $y = 1$; and
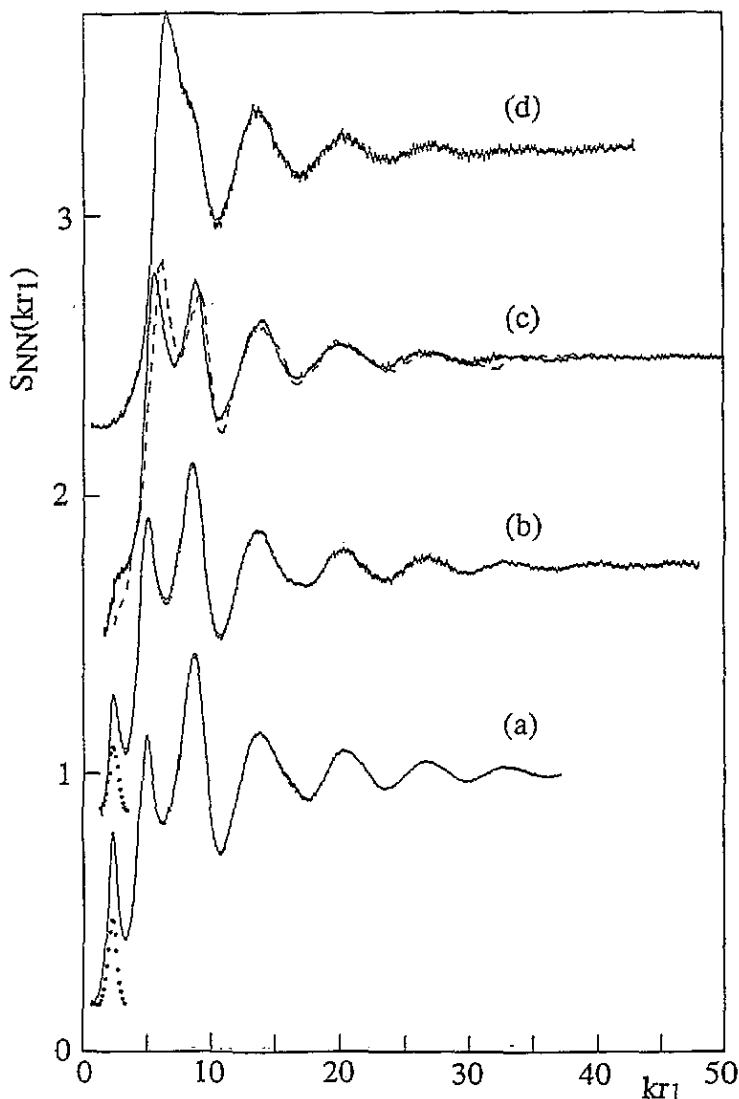
Figure 1. The measured $S_{NN}(k)$ functions for liquid Ge_ySe_{1-y} alloys plotted as a function of kr_1, where r_1 is the position of the first peak in $g_{NN}(r)$ (see table 2): curve a, $Ge_{0.33}Se_{0.67}$; curve b, $Ge_{0.40}Se_{0.60}$; curve c, $Ge_{0.50}Se_{0.50}$; curve d, Ge. The $S_{NN}(kr_1)$ for (b), (c) and (d) are shifted vertically by values of 0.75, 1.5 and 2.25, respectively. The vertical lines give the statistical error on a data point and the solid curves give the Fourier back transform of the corresponding $g_{NN}(r)$ functions of figure 2 after the unphysical oscillations at low r are set to their calculated limiting value. The solid curves are nearly identical with the minimum information method (MIM) k-space solutions. The dotted curves a and b give the FSDP obtained by a linear interpolation between points in $S_{NN}(k)$ deemed to mark the start and end of a FSDP. The dashed curve in c gives $S_{NN}(kr_1)$ for liquid As where $r_1 = 2.50$ Å (Bellissent *et al* 1987, Howe *et al* 1993).

the amplitude of the high-k oscillations is reduced. These features also show that there is an alteration to the character of the bonding. For example, the loss of the FSDP indicates a change in its directionality (Salmon 1992) while the damping of the high-k oscillations indicates a break-up of the local structural motifs. Thus the three-peak character of $S_{NN}(k)$
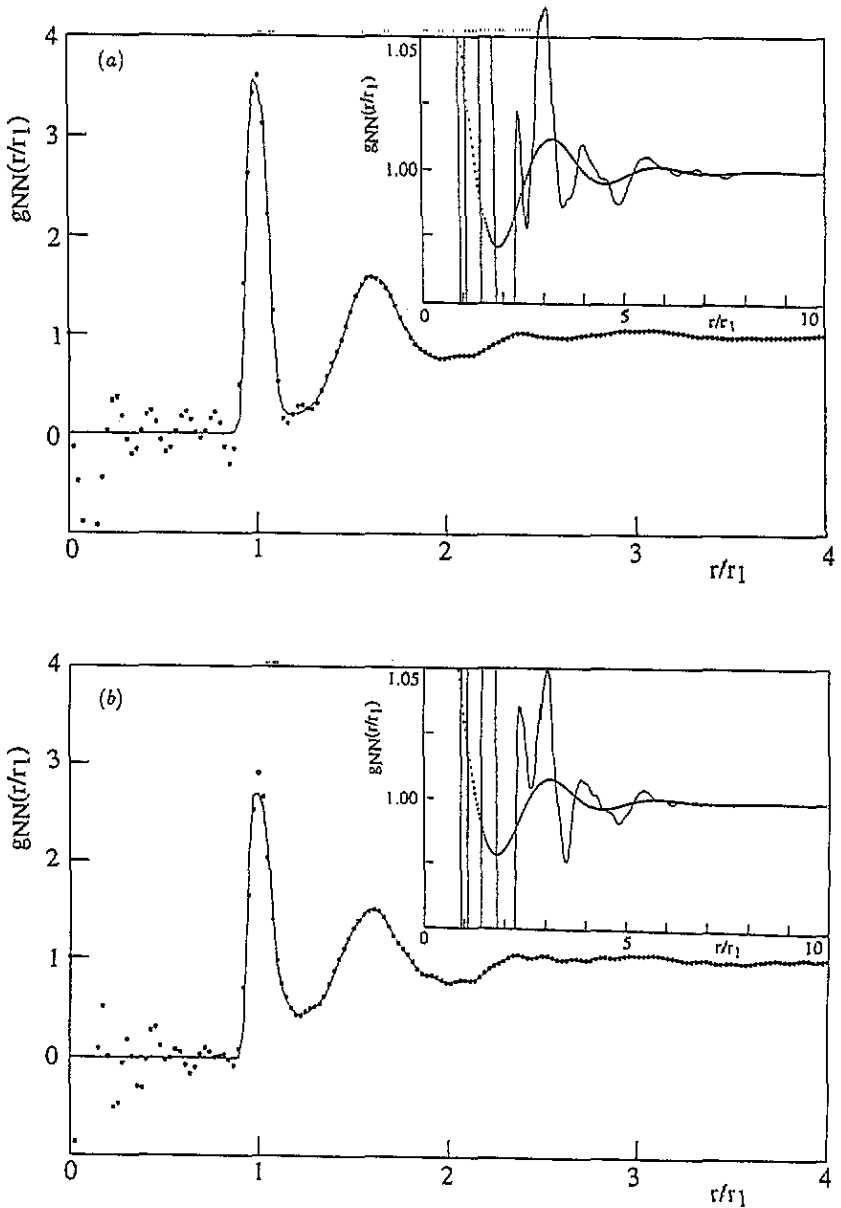
Figure 2. $g_{NN}(r)$ plotted as a function of r/r_1, where r_1 is the position of its first peak (see table 2): (a) $Ge_{0.33}Se_{0.67}$; (b) $Ge_{0.40}Se_{0.60}$; (c) $Ge_{0.50}Se_{0.50}$; (d) Ge. The points give the result of Fourier transforming $S_{NN}(k)$ represented by the vertical lines in figure 1 and the solid curves give the MIM solutions. The insets to (a) and (b) compare $g_{NN}(r/r_1)$ (MIM solution given by the solid curve) with the Fourier transform, $I(r_1)$, (dotted curve) of the FSDP in $S_{NN}(k)$ (see text for details). The positions of the vertical bars in (c) give the nearest-neighbour interaction distance (divided by $r_1 = 2.51$ Å) in the low-temperature form of crystalline GeSe (which has a 3 + 3 conformation) and their height is proportional to the number of atoms. The dashed curve in (c) gives $g_{NN}(r/r_1)$ for liquid As.

is progressively destroyed as $y \to 1$. It is noteworthy that the profile of $S_{NN}(k)$ at $y = 0.5$ is significantly different from the form characteristic of a simple 1:1 ionic salt such
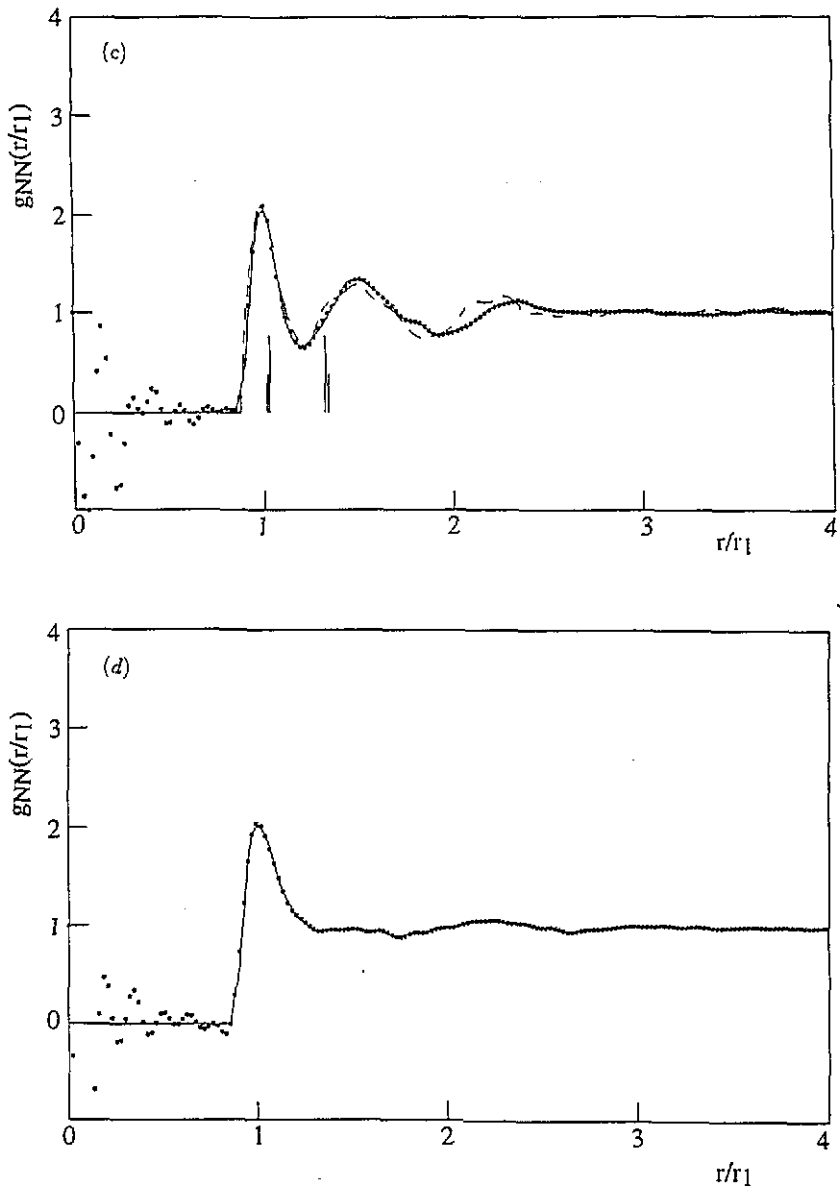
Figure 2. Continued.

as NaCl (Rovere and Tosi 1986) and is different from that for a 1:1 system such as CuCl which melts from a superionic phase (Eisenberg *et al* 1982). It is, however, very similar to $S_{NN}(k)$ for liquid As at 825 °C and 47 atm (Bellissent *et al* 1987, Howe *et al* 1993) as shown in figure 1, curve c.

5.2. Short-range order

The two crystalline compounds that form in the Ge–Se system are $GeSe_2$ and GeSe (Ipser *et al* 1982). The former of these melts congruently at 742(2) °C and the full set of partial

Table 2. Parameters describing the $S_{NN}(k)$ and $g_{NN}(r)$ functions for molten Ge–Se systems. r_1 is the position of the first peak in $g_{NN}(r)$. $\bar{n}$ was calculated (equation (8)) by integrating over the specified region to the first minimum in $r^2 g_{NN}(r)$. The same integration range was used to calculate $\bar{n}_{Ge}^{Se}$ (equation (7)) on the assumption that the first peak in $g_{NN}(r)$ is dominated by $g'_{GeSe}(r)$ (see text). k_ϵ (ϵ = 1, 2, 3 or 4) denotes the position of a peak in $S_{NN}(k)$ and $S_{NN}(k_\epsilon)$ gives the corresponding value of this function. The Fourier transform and MIM solutions give coordination numbers in agreement within the quoted error margins.

Melt	r_1 (Å)	$\bar{n}$	$\bar{n}_{Ge}^{Se}$	k_2 (Å^{-1})	k_1/k_2	k_3/k_2	k_4/k_2
GeSe$_2$	2.38(2)	2.6(1)	3.8(2)	2.02(3)	0.49	1.75	2.75
		(2.08 $\leqslant$ r (Å) $\leqslant$ 2.76)					
GeSe$_{1.5}$	2.41(2)	2.8(2)	3.5(2)	2.08(3)	0.47	1.70	2.67
		(2.15 $\leqslant$ r (Å) $\leqslant$ 2.95)					
GeSe	2.51(2)	3.6(3)	3.6(3)	2.22(3)	0.50	1.56	2.50
		(2.15 $\leqslant$ r (Å) $\leqslant$ 3.07)					
Ge	2.66(2)	5.8(4)	—	2.48(3)	—	$\simeq$ 1.25	2.06
		(2.25 $\leqslant$ r (Å) $\leqslant$ 3.19)					

Melt	$S_{NN}(k_2)$	$S_{NN}(k_1)/S_{NN}(k_2)$	$S_{NN}(k_3)/S_{NN}(k_2)$	$S_{NN}(k_4)/S_{NN}(k_2)$
GeSe$_2$	1.125(4)	0.694	1.258	1.018
GeSe$_{1.5}$	1.166(3)	0.453	1.160	0.964
GeSe	1.298(4)	0.174	0.981	0.875
Ge	1.49(1)	—	0.78	0.76

structure factors for the melt has been measured using the method of isotopic substitution in neutron diffraction (Penfold and Salmon 1991). The results show that the liquid retains a memory, at both the short and intermediate length scales, of the high-temperature crystalline form of GeSe$_2$, which has a layer-type structure (Von Dittmar and Schäfer 1976). The liquid comprises roughly equal numbers of edge- and corner-sharing Ge(Se$_{1/2}$)$_4$ tetrahedra, which are connected to form a viscous network. The first peak in $g_{GeSe}(r)$ at 2.42(2) Å is well defined and gives a coordination number $\bar{n}_{Ge}^{Se}$ = 3.6(3). These parameters are, within experimental error, in agreement with those obtained from the first peak in $g_{NN}(r)$ (table 2) and therefore support the interpretation of this feature for GeSe$_2$ as arising predominantly from the Ge–Se correlations.

The first peak in $g_{NN}(r)$ for y = 0.4 will, on the basis of the '8–N' rule, comprise both Ge–Se and Ge–Ge correlations. It is not possible to unambiguously identify the relative contributions from these correlation functions on the basis of the present data. However, Zhou *et al* (1991) deduced from their EXAFS data on bulk-quenched Ge$_{0.40}$Se$_{0.60}$ that $\bar{n}_{Ge}^{Se}$ = 3.0(3) and $\bar{n}_{Ge}^{Ge}$ = 1.0(2) (see table 3). If the first peak in $g_{NN}(r)$ is analysed assuming $\bar{n}_{Ge}^{Se}$ = 3.0(3), a value for $\bar{n}_{Ge}^{Ge}$ = 1.0(5) is also obtained from the liquid-state data.

As y increases to 0.5 the first peak in $g_{NN}(r)$ continues to decrease in magnitude and its position shifts towards higher r values (table 2). Furthermore, the height of the minimum after the first peak increases, which makes for a larger uncertainty in the value of the coordination number. However, if it is assumed that the first peak results predominantly from hetero-polar contacts, a value $\bar{n}_{Ge}^{Se} \ll$ 6 is obtained. This is significant since GeSe, which melts incongruently at 675(2) °C (Ipser *et al* 1982), is reported to undergo a structural phase transition at 651(5) °C. Below this temperature GeSe forms a distorted NaCl-type structure in which each chemical species forms three strong and three weak bonds to unlike species to give a double-layer structure (Okazaki 1958, Kannewurf *et al* 1960, Dutta and Jeffrey 1965, Hulliger 1976). Above the transition temperature a normal NaCl-type structure is reported to occur (Wiedemeier and Siemers 1975). However, the data for the molten state

Table 3. Parameters obtained for the structure of liquid and glassy Ge_ySe_{1-y} alloys. r'_1 and r'_2 refer to the first and second peak positions in either $rg_{NN}(r)$ or $r^2g_{NN}(r)$.

Sample	r'_1 (Å)	r'_2/r'_1	$\tilde{n}$	Technique	Preparation method	Reference
$Ge_{0.33}Se_{0.67}$	2.39(2)	1.607	2.6(1)	Neutron	Liquid at 784 °C	present work
$Ge_{0.40}Se_{0.60}$	2.41(2)	1.618	2.8(2)	—	Liquid at 728 °C	—
$Ge_{0.50}Se_{0.50}$	2.52(2)	1.520	3.6(3)	—	Liquid at 728 °C	—
$Ge_{0.33}Se_{0.67}$	2.40	1.621	2.16	Neutron	Liquid at 811 °C	Susman *et al* (1990)
	2.385	1.648	2.74	—	Melt quenched	—
$Ge_{0.33}Se_{0.67}$	2.40(5)	1.628	2.8	Neutron	Liquid at 771 °C	Uemura *et al* (1978)
	2.365	1.632	2.62	Neutron	Melt quenched	Uemura *et al* (1975)
$Ge_{0.33}Se_{0.67}$	2.35	1.647	2.6	X-ray	Melt quenched	Satow *et al* (1973)
$Ge_{0.395}Se_{0.605}$	2.34	1.641	2.5	—	—	—
$Ge_{0.40}Se_{0.60}$	2.39(1)	1.619	2.7(2)	X-ray	Melt quenched	Malaurent and Dixmier (1980)
$Ge_{0.33}Se_{0.67}$	2.364(5)[a]	—	2.5(2)	EXAFS	Melt quenched	Zhou *et al* (1991)
$Ge_{0.37}Se_{0.63}$	2.365(5)[a] 2.44(2)[b]	—	2.7(3)	—	—	—
$Ge_{0.40}Se_{0.60}$	2.365(5)[a] 2.41(2)[b]	—	2.7(3)	—	—	—
$Ge_{0.50}Se_{0.50}$	2.35 & 2.80	—	~3	EXAFS	Evaporated	Sayers *et al* (1972)
$Ge_{0.50}Se_{0.50}$	2.44	1.597	2.8	DAS	Sputtered	Fuoss *et al* (1981)
$Ge_{0.32}Se_{0.68}$	2.3(1)	1.609	2.6(5)	Electron	Evaporated	Fawcett *et al* (1972)
$Ge_{0.56}Se_{0.44}$	2.3(1)	1.522	2.5(5)	Electron	—	—
$Ge_{0.59}Se_{0.41}$	2.4	1.833	2.5	Electron	Evaporated	Molnar and Dove (1974)
$Ge_{0.33}Se_{0.67}$	2.34(2)	1.620	2.63	Electron	Evaporated	Uemura *et al* (1974)
$Ge_{0.40}Se_{0.60}$	2.38(2)	1.613	2.7	—	—	—
$Ge_{0.50}Se_{0.50}$	2.40(2)	1.600	2.8	—	—	—

[a] r_{GeSe}.

[b] r_{GeGe}.

are *not* consistent with the structure of the high-temperature GeSe phase since the measured coordination number is too low.

The similarity between the measured $S_{NN}(k)$ for liquid GeSe and As (figure 2(c)) is significant since the crystal structures of these materials are related. Structures of the As and GeTe type arise from a rhombohedral distortion of the rocksalt structure while structures of the black phosphorus and (low-temperature) GeSe type arise from a quasi-tetragonal deformation (Hulliger 1976). Furthermore, whereas the atomic arrangement in crystalline GeSe more closely resembles that of black phosphorus, the atomic bonding is closer to that of As (Dutta and Jeffrey 1965) and r_1 for liquid GeSe is very similar to the nearest-neighbour interaction distances in the crystalline GeSe phase (see figure 2(c)). The neutron-diffraction results for molten GeSe are therefore better described in terms of the structure of the *low*-temperature crystalline phase. Indeed, the similarity between the $g_{NN}(r)$ functions for the GeSe and As liquids and the comparability of their number densities (As is 8% more dense) shows that these structures are topologically similar at the level of the pair distribution function.

Both the number density, n_0, (table 1) and mean coordination number, $\tilde{n}$, (table 2) increase as $y \to 1$. The latter quantity can be compared with that calculated on the basis of the so-called random covalent model (RCM) where, by the '8–N' rule, the coordination numbers of Ge and Se are, respectively, four and two and homo-polar Ge–Ge bonds are allowed (Betts *et al* 1970). Equation (8) then gives $\tilde{n} = 2.67$ ($y = 0.33$), 2.80 ($y = 0.4$), 3 ($y = 0.5$) and 4 ($y = 1$). The first two values are, within the estimated error, in agreement with experiment. Also, the measured partial structure factors for liquid $GeSe_2$ (Penfold and Salmon 1991) are consistent with Ge being predominantly fourfold coordinated by Se

and the present results for liquid GeSe$_{1.5}$ can be interpreted in terms of each Ge being surrounded by an average of three Se and one Ge. The RCM is therefore consistent with the $y = 0.33$ and $y = 0.4$ results. However, the model is not valid for $y = 0.5$ since the liquid data are best described by a model in which Ge and Se are *both* threefold coordinated. Furthermore, although crystalline and amorphous Ge are semi-conductors that have a tetrahedral coordination environment (Etherington *et al* 1982), liquid Ge is a metal for which the local ordering is relatively ill defined and for which $\bar{n} > 4$ (table 2). Suggestions for the local conformation in the liquid include a distorted white-tin structure where four nearest neighbours are at the corners of a flattened tetrahedron and two others are at a slightly greater distance (Isherwood *et al* 1972); a collapsed diamond structure in which there is overlap between the first (four atom) and second (12 atom) coordination shells (Howe *et al* 1993); and a model in which the melt comprises transient Ge$_4$ clusters identifiable for a timescale comparable with that required for diffusive motion (Ashcroft 1990).

5.3. Intermediate-range order

If the FSDP in $S_{NN}(k)$ is treated as a distinct feature it can be shown using Fourier transform theory that its position, k_1, gives rise to oscillations in r space of periodicity $2\pi/k_1$ and that its shape controls the modulation of these oscillations (Salmon 1994). For example, a narrow peak will give rise to a slow decay of the oscillations in r space and a high peak will give rise to oscillations of large amplitude. $I(r)$, the Fourier transform of the FSDP as derived from a linear interpolation between points deemed to mark the start and end of the peak, is given in figure 2(a) and (b) for the $y = 0.33$ and $y = 0.4$ compositions, respectively. Different interpolation schemes were not used since the peak is clearly defined and no substantial change in the results is therefore expected (Salmon 1994). The comparison of figure 2 shows that $I(r)$ describes the underlying features of the observed IRO. This ordering decreases in amplitude, but has little change in range or periodicity, as y increases from 0.33 to 0.4: the FSDP in $S_{NN}(k)$ at these two compositions has values of position, full width at half maximum and height of 0.98(5) Å^{-1}, 0.33(1) Å^{-1}, 0.473(4) and 0.98(5) Å^{-1}, 0.34(1) Å^{-1}, 0.351(4) respectively.

The measured $A_{\alpha\beta}(k)$ for liquid GeSe$_2$ (Penfold and Salmon 1991) show that the FSDP arises predominantly from the Ge–Ge correlations, i.e. from the relative positions of the Ge(Se$_{1/2}$)$_4$ tetrahedron centres. The loss of the FSDP and concomitant elimination of the associated IRO with increasing y is thus in accordance with a change in the nature of the bonding, which leads to a break-up of the GeSe$_2$ network structure and a denser packing (see table 1) of atoms.

5.4. Comparison with the structure of the amorphous phase of Ge$_y$Se$_{1-y}$ alloys

It is of interest to investigate the extent to which the topology of the molten and glassy phases of Ge$_y$Se$_{1-y}$ alloys is similar and to ask whether the structure of the melt resembles that of amorphous Ge$_y$Se$_{1-y}$ alloys not prepared by bulk quenching methods.

Uemura *et al* (1978) and Susman *et al* (1990) have studied molten and glassy GeSe$_2$ by neutron diffraction and found that the general form of the measured $S_{NN}(k)$ is the same. A comparison of some of the results is given in table 3. X-ray diffraction and electron diffraction techniques have been applied to study the composition dependence of, respectively, bulk quenched (Satow *et al* 1973, Malaurent and Dixmier 1980) and evaporated (Fawcett *et al* 1972, Molnar and Dove 1974, Uemura *et al* 1974) Ge$_y$Se$_{1-y}$ alloys. Since the atomic numbers of Ge and Se are comparable, the diffraction experiments yield total

structure factors also dominated by $S_{NN}(k)$. The measured patterns for the bulk quenched glasses and amorphous evaporated alloys (when $y \leqslant 0.42$) all show the characteristic three-peak structure for $0 \leqslant kr_1 \leqslant 10$. Furthermore, for a given composition, there is fair agreement between the real-space peak positions and $\tilde{n}$ values, a similar finding being made when EXAFS results for bulk-quenched Ge_ySe_{1-y} alloys (Zhou *et al* 1991) are compared with those obtained for the liquid state.

As for the liquid state the FSDP for evaporated or sputtered amorphous GeSe is much weaker than for compositions near $GeSe_2$ (Molnar and Dove 1974, Uemura *et al* 1974, Fuoss *et al* 1981). Also, x-ray differential anomalous scattering (DAS) experiments on sputtered amorphous GeSe samples are consistent with a 3–3 model in which both Ge and Se are threefold coordinated (Fuoss *et al* 1981). However, the nearest-neighbour distance in the amorphous phase is smaller than that in the melt ($\simeq 2.4$ Å cf 2.52 Å) and the coordination number is reduced ($\tilde{n} \simeq 2.8$ cf 3.6). Indeed, the local ordering of the low-temperature GeSe phase more closely resembles that of the liquid (see section 5.2) rather than the amorphous (Sayers *et al* 1972, Bienenstock 1973, Molnar and Dove 1974) state. In accordance with the metallic and semi-conducting natures of, respectively, the molten and amorphous phases of Ge their structures are somewhat different (see e.g. Wright *et al* 1991).

6. Conclusions

The change in the topology of liquid Ge_ySe_{1-y} over the composition range $0.33 \leqslant y \leqslant 1$ is significant and is clearly visible in both real and reciprocal spaces. The $y = 0.33$ and $y = 0.4$ alloys form glasses by bulk-quenching methods and are characterized by a function $S_{NN}(kr_1)$, which has a three-peak structure for $0 \leqslant kr_1 \leqslant 10$. The FSDP is virtually absent at $y = 0.5$, which lies outside the glass-forming region, and the third peak becomes a shoulder to the second at $y = 1$. Both the average coordination number, $\tilde{n}$, and nearest-neighbour distance, r_1, increase as $y \to 1$, giving rise to a progressively closer-packed structure. Accompanying this trend is an elimination of the underlying density oscillations that arise from the FSDP and which are a characteristic feature of the $GeSe_2$ network structure.

Acknowledgments

References

Ashcroft N W 1990 *Nuovo Cimento* D **12** 597
Azoulay R, Thibierge H and Brenac A 1975 *J. Non-Cryst. Solids* **18** 33
Bellissent R, Bergman C, Ceolin R and Gaspard J P 1987 *Phys. Rev. Lett.* **59** 661
Betts F, Bienenstock A and Ovshinsky S R 1970 *J. Non-Cryst. Solids* **4** 554
Bhatia A B and Thornton D E 1970 *Phys. Rev.* B **2** 3004
Bienenstock A 1973 *J. Non-Cryst. Solids* **11** 447
Blank H and Maier B (ed) 1988 *Guide to Neutron Research Facilities* (Grenoble: Institut Laue Langevin)
Dutta S N and Jeffrey G A 1965 *Inorg. Chem.* **4** 1363
Eisenberg S, Jal J-F, Dupuy J, Chieux P and Knoll W 1982 *Phil. Mag.* A **46** 195

Etherington G, Wright A C, Wenzel J T, Dore J C, Clarke J H and Sinclair R N 1982 *J. Non-Cryst. Solids* **48** 265

Fawcett R W, Wagner C N J and Cargill G S III 1972 *J. Non-Cryst. Solids* **8–10** 369

Feltz A, Pohle M, Steil H and Herms G 1985 *J. Non-Cryst. Solids* **69** 271

Fischer-Colbrie A and Fuoss P H 1990 *J. Non-Cryst. Solids* **126** 1

Fuoss P H, Eisenberger P, Warburton W K and Bienenstock A 1981 *Phys. Rev. Lett.* **46** 1537

Fuoss P H and Fischer-Colbrie A 1988 *Phys. Rev.* B **38** 1875

Glazov V M and Situlina O V 1969 *Dok. Chem.* **187** 587

Grimley D I, Wright A C and Sinclair R N 1990 *J. Non-Cryst. Solids* **119** 49

Haisty R W and Krebs H 1969 *J. Non-Cryst. Solids* **1** 399

Howe M A, McGreevy R L, Pusztai L and Borzsák I 1993 *Phys. Chem. Liquids* **25** 205

Hulliger F 1976 *Physics and Chemistry of Materials with Layered Structures* vol 5, ed F Lévy (Dordrecht: Reidel)

Ipser H, Gambino M and Schuster W 1982 *Monat. Chem.* **113** 389

Isherwood S P, Orton B R and Mănăilă R 1972 *J. Non-Cryst. Solids* **8–10** 691

Jal J F, Mathieu C, Chieux P and Dupuy J 1990 *Phil. Mag.* B **62** 351

Kannewurf C R, Kelly A and Cashman R J 1960 *Acta Crystallogr.* **13** 449

Malaurent J C and Dixmier J 1980 *J. Non-Cryst. Solids* **35 & 36** 1227

Molnar B J and Dove D B 1974 *J. Non-Cryst. Solids* **16** 149

Okazaki A 1958 *J. Phys. Soc. Japan* **13** 1151

Parrinello M and Tosi M P 1979 *Riv. Nuovo Cimento* **2** 1

Penfold I T and Salmon P S 1989 *J. Non-Cryst. Solids* **114** 82

—— 1990 *J. Phys.: Condens. Matter* **2** SA233

—— 1991 *Phys. Rev. Lett.* **67** 97

Price D L, Moss S C, Reijers R, Saboungi M-L and Susman S 1988 *J. Phys. C: Solid State Phys.* **21** L1069

Rovere M and Tosi M P 1986 *Rep. Prog. Phys.* **49** 1001

Ruska J and Thurn H 1976 *J. Non-Cryst. Solids* **22** 277

Salmon P S 1988 *J. Phys. F: Met. Phys.* **18** 2345

—— 1992 *Proc. R. Soc.* A **437** 591

—— 1994 *Proc. R. Soc.* at press

Salmon P S and Benmore C J 1992 *Recent Developments in the Physics of Fluids* ed W S Howells and A K Soper (Bristol: Adam Hilger) p F225

Satow T, Uemura O and Sagara Y 1973 *Japan. J. Inst. Met.* **37** 1348

Sayers D E, Lytle F W and Stern E A 1972 *J. Non-Cryst. Solids* **8–10** 401

Sears V F 1992 *Neutron News* **3** 26

Soper A K 1990 *Neutron Scattering Data Analysis (Inst. Phys. Conf. Ser. 107)* ed M W Johnson (Bristol: Institute of Physics Publishing) p 57

Soper A K, Howells W S and Hannon A C 1989 *Rutherford Appleton Laboratory Report* RAL-89-046

Susman S, Volin K J, Montague D G and Price D L 1990 *J. Non-Cryst. Solids* **125** 168

Tronc P, Bensoussan M, Brenac A and Sebenne C 1973 *Phys. Rev.* B **8** 5947

Tsuchiya Y 1990 *J. Non-Cryst. Solids* **122** 205

Uemura O, Sagara Y, Muno D and Satow T 1978 *J. Non-Cryst. Solids* **30** 155

Uemura O, Sagara Y and Satow T 1974 *Phys. Status Solidi* a **26** 99

—— 1975 *Phys. Status Solidi* a **32** K91

—— 1976 *Trans. Japan. Inst. Met. Qouy* **17** 457

Von Dittmar G and Schäfer H 1976 *Acta Crystallogr.* B **32** 2726

Wiedemeier H and Siemers P A 1975 *Z. Anorg. (Allg.) Chem.* **411** 90

Wright A C, Hulme R A, Grimley D I, Sinclair R N, Martin S W, Price D L and Galeener F L 1991 *J. Non-Cryst. Solids* **129** 213

Wright A C, Sinclair R N and Leadbetter A J 1985 *J. Non-Cryst. Solids* **71** 295

Zhou W, Paesler M and Sayers D E 1991 *Phys. Rev.* B **43** 2315